Design and Preliminary Validation of a Lightweight Powered Exoskeleton During Level Walking for Persons With Paraplegia

Duojin Wang, Bingshan Hu, Wenming Chen, *Member, IEEE*, Qingyun Meng, Shiyu Liu, Suowen Ma, Xinwei Li, and Hongliu Yu

***Abstract*— Upright-legged locomotion is a desirable ability for people with paraplegia. This paper introduces a newly developed lightweight powered exoskeleton (LIPE) for level walking and posture transfer of people with paraplegia using a user-centered design concept, which integrates the requirements of practical use, mechanical structure, and control system. The LIPE was evaluated with two subjects through several experimental tasks including kinematics and dynamics analysis in a local hospital. Results of functional evaluation showed that these subjects received the exoskeleton intervention well and the LIPE could provide appropriate gait assistance to the wearer during level walking, it could also help the wearer achieve the posture transfer from sitting to standing or from standing to sitting independently. Moreover, an endurance test also indicated that LIPE allows wearers to use it continuously for a long time. It is lightweight, cost effective, easy to use, and practical for people with paraplegia in their daily lives.**

***Index Terms*— Lightweight, exoskeleton, level walking, paraplegia.**

I. Introduction

PEOPLE with paraplegia caused by spinal cord injury expect to walk again. However, many of them cannot achieve independent standing or walking ability after rehabilitation [1]. Generally, they are forced to use a wheelchair for mobility in activities of daily living (ADL). Research has shown that long-term wheelchair dependence can entail significant health implications, including pressure sores, osteoporosis, muscle spasticity, constipation, obesity [2], even increased incidence of urinary tract infection, impaired lymphatic and vascular circulation, and reduced respiratory and cardiovascular capacities [3]. In addition, non-eye-level communication with others in a wheelchair leads to a significant psychological gap [4]. Therefore, seeking suitable ways to facilitate upright-legged locomotion is a key issue for individuals with paraplegia.

At present, a number of lower limb orthoses systems/exoskeletons have been or are being developed, of which several mature products have been launched.

On the academic side, some studies present some noteworthy features, which could have a significant impact on the devices' performance. The most representative of this type of exoskeleton include Mina [5], ALEX-1 [6], ATLAS [7], BLERE [8], p-EXO [9], IRGO [10], MME [12], WPAL [13], WSE [14], HAL-5 [15], TWIICE [16], CUHK-EXO [17], THU-LLE [18] and PAWE [19]. They could assist people with spinal cord injury (SCI) to implement ambulation training over the ground or to achieve active walking. In these studies, the exoskeleton wearers used two forearm crutches or walkers to provide a significant support polygon for locomotion. It is worth noting that the PAWE walks with wheeled feet, while in other studies, the exoskeletons walk by stepping.

So far, among exoskeletons for full mobilization are also several commercial products, already available for purchase, like HAL [20], ReWalk [21], Ekso GT [22], Rex [23], Indego [24], PHOENIX [25], ATALANTE [26], Fourier X2 [27], AiLegs [28] and UGO [29]. However, there is often limited information available about these devices due to their commercialization. Nevertheless, it can be seen from the open information that REX and ATALANTE are remarkable in that they are self-stabilizing without requiring crutches. This frees the user's hands but comes at the cost of an extremely low walking speed and an increased overall weight.

Manuscript received May 31, 2021; revised August 13, 2021 and September 24, 2021; accepted October 5, 2021. Date of publication October 8, 2021; date of current version October 28, 2021. This work was supported by the Shanghai Science and Technology Innovation Action Plan under Grant 19DZ2203600. *(Corresponding author: Hongliu Yu.)*

This work involved human subjects or animals in its research. Approval of all ethical and experimental procedures and protocols was granted by the Institutional Review Committee of the Shanghai University of Medicine and Health Sciences under Approval No. 2019-ZYXM1-04-420300197109053525.

Duojin Wang, Bingshan Hu, Shiyu Liu, Suowen Ma, Xinwei Li, and Hongliu Yu are with the Institute of Rehabilitation Engineering and Technology, University of Shanghai for Science and Technology, Shanghai 200093, China, and also with the Shanghai Engineering Research Center of Assistive Devices, Shanghai 200093, China (e-mail: duojin.wang@usst.edu.cn; icebergh@126.com; nssmail@163.com; msw18136243900@sina.com; lixinwei0806@163.com; ichbinotto@aliyun.com).

Wenming Chen is with the Academy for Engineering and Technology, Fudan University, Shanghai 200433, China (e-mail: chenwm@fudan.edu.cn).

Qingyun Meng is with the College of Rehabilitation Sciences, Shanghai University of Medicine and Health Sciences, Shanghai 201318, China (e-mail: mengqy1996@126.com).

This article has supplementary downloadable material available at https://10.1109/TNSRE.2021.3118725, provided by the authors.

Digital Object Identifier 10.1109/TNSRE.2021.3118725

TABLE I
REVIEW OF LOWER LIMB ORTHOSES SYSTEMS /EXOSKELETONS FOR RESTORATION OF GAIT

Products/ systems	Developer	Weight (kg)	Total DOF	Hip DOF	Knee DOF	Ankle DOF	Actuators	Low-level controller, Parameter	Status
Mina	IHMC	–	4	E-U-U	E	U-U-U	BLDC motor	PD controller, Torque	R
ALEX-1	AIT	–	12	E-E-E	E	E-E-U	DC motor	PID controller, Angle	R
ATLAS	CSIC	6.5	6	E-U-U	E	P-U-U	Electric brushless motor	Impedance controller, -	R
BLERE	ZJU	–	8	E-P-P	E	F-F-F	Servomotor	Not mentioned	R
p-EXO	Salford	–	10	Pn- Pn- Pn	Pn	Pn-U-U	Pneumatic Muscle Actuator	PID controller, Pressure	R
IRGO	USWR	10.1	4	E-U-U	E	U-U-U	Maxon motor	Not mentioned	R
MINDWALK ER	TU Delft	28	12	H-H-P	H	P-P-U	Series elastic actuator	Impedance controller, Torque	R
MME	MU	–	9	F-U-U	H	H-F-U	Electrical motor & spring	Not mentioned	R
WPAL	Fujita-HU	13	6	E-F-F	E	E-U-U	BLDC servomotor	Not mentioned	R
WSE	NEU	15	4	E-U-U	E	U-U-U	Servomotor	Fuzzy logic controller, Angular positions	R
HAL-5	Cyberdyne	–	6	E-U-U	E	E-U-U	DC Servomotor	PD controller, Joint angle	R
TWIICE	EPFL	15	4	E-U-U	E	U-U-U	BLDC motor	PI & PD controllers, Position	R
CUHK-EXO	CUHK	–	7	E-U-U	E	P-U-U	DC motor	PD controller, Torque	R
THU-LLE	THU	–	6	E- U-U	E	P-U-U	DC motor	PID controller, Position	R
PAWE	THU	–	6	P-U-U	M	P-U-U	Hub motor	Not mentioned	R
Med-HAL	Cyberdyne	–	6	E-U-U	E	P-U-U	DC Servomotor	Not mentioned	C
ReWalk	ReWalk Robotics	23	6	E-U-U	E	P-U-U	DC motor	Not mentioned	C
Ekso GT	Ekso Bionics	28	6	E-U-U	E	P-U-U	Electrical motor & spring	Not mentioned	C
Rex	Rex Bionics	38	10	E-E-U	E	E-E-U	Brushed DC motors	Not mentioned	C
Indego	Parker Hannifin	11.8	4	E-U-U	E	U-U-U	BLDC motor	PD controller, Torque	C
PHOENIX	SuitX	12.3	4	E-U-U	P	U-U-U	Electrical motor	Not mentioned	C
ATALANTE	Wandercraft	59	12	E-E-E	E	P-P-U	Electrical motor	feedback-linearizing controller, Position	C
Fourier X2	Fourier	18	6	E-U-U	E	P-U-U	Servomotor	Not mentioned	C
AiLegs	Ai-Robotics	20	4	E-U-U	E	U-U-U	Servomotor	Not mentioned	C
UGO 210	ToboCT	–	6	E-U-U	E	P-U-U	Servomotor	Not mentioned	C

NOTE: E – Electric motor. U – Unactuated. Pn – Pneumatic. P – Passive. H – Hybrid. F – Freely. M – Manually. Hip joint DOF - (Flexion/Extension, Abduction/Adduction, Internal/External Rotation). Knee joint DOF – (Flexion/Extension). Ankle joint DOF – (Plantar/Dorsal Flexion, Inversion/Eversion, Internal/External Rotation). R – Research stage. C – Commercial stage.

TABLE 1 presents the comparative review of popular lower limb exoskeletons intended for level walking for persons with paraplegia.

As TABLE 1 shows, the actuators of the such exoskeletons mainly include electrical motor, pneumatic, and series elastic drive at present. Each actuator has its own advantages, but because the motor drive can achieve accurate position control which is difficult to complete by pneumatic and hydraulic drive, it has become a common driving method for such devices. From another perspective, the current motors involved in such research and products are relatively large and heavy while having a small torque, the high-performance motor, therefore, is likely to be one of the directions of such research. In addition, the control method, especially the intent detection for physical human–robot interaction, is also one of the important factors affecting the development of wearable exoskeleton robot [30]. Researchers are pursuing better real-time and more stable control methods. Finally, high endurance and lightweight structure are also hot topics of research.

The development of the lower limb exoskeleton actually needs to balance the functionality, endurance, portability, and cost of the product. However, we know from the above literature review that the current related products are either too large, too expensive, or have poor endurance, which cannot be in a relatively balanced state. Therefore, this paper attempts to develop a lightweight powered exoskeleton (LIPE) during level walking for people with paraplegia with the aim of ensuring functionality while maintaining long-lasting battery life and simpler structure to improve product availability.

In what follows, we describe the design requirements and solutions (Section II). Then experimental tasks are presented in Section III, and followed by the discussion and conclusion.

II. Materials and Methods

The system performance requirements for a wearable lower limb exoskeleton are user-centered and grouped into two main categories: practical considerations and technical requirements. These requirements were obtained from a combination of review on the literature, experimental studies, and discussions with a multidisciplinary group, which include designers, users, and physical/occupational therapists, etc.

A. Practical Considerations

The practical design requirements are summarized in TABLE 2.

Safety is the first issue to consider in our design. Compared to the walkers, we use two forearm crutches to provide

TABLE II
PRACTICAL CONSIDERATIONS OF LIPE

Characteristic	Requirements
Walking manner	Quadrupedal gait with forearm crutches
Fit with different wearers	Adjustable size
Lightweight	<15kg
Long endurance	Continuous walking time ⩾4 hours
Use pattern	Level walking & sit-to-stand/stand-to-sit

TABLE III
TECHNICAL REQUIREMENTS OF LIPE

Characteristic		Requirements
Lightweight, long endurance		1 power DOF per leg at hip joint
Total DOFs per leg		5
ROM	Hip flexion/extension	~120°/~20°
	Hip adduction/abduction	~15°/~15°
	Hip external/internal Rotation	~30°/~30°
	Knee flexion/extension	~120°/~0°
	Ankle plantar/dorsal flexion	~30°/~15°
Walking speed		~0.6m/s
Walking gait		Good symmetry
Control mode		Manually switch with push-button interface

a significant support polygon for the wearer, which could produce more of a static quadrupedal gait and keep the wearer in balance. Considering the different heights of wearers, adjustable shank and thigh segments of the exoskeleton might be a more convenient choice, while avoiding the high cost of individual customization. Lightweight and long endurance under the premise of ensuring functionality has always been the goal pursued by all designers of lower limb exoskeleton. Therefore, after analyzing the existing research and products shown in TABLE 1, we believe a maximum weight of 15 kg is feasible. Four-hour battery life while in continuous use is the level of individual existing products; we used it as a benchmark for longer walking distances or durations. The sitting position is conducive to don and doff the device, so the use pattern includes level walking and switching between sitting and standing.

B. Technical Requirements

As shown in TABLE 3, the technical requirements involve some specific parameter information.

LIPE's mechanical design was driven by one major rule: simplicity. The key idea behind it was to reduce the number and complexity of features for the benefit of reliability and lightness. In a complete level walking gait cycle, the greatest energy expenditure is the hip flexion/extension, while the knee joint performs negative work most of the time. Ankle push-off power burst provides energy for swing initiation; the plantar flexors also have an important support function [31]. Therefore, to support the wearer to maintain balance in both sagittal and frontal planes, the minimum requirement, namely hip flexion/extension of each leg, is required to be powered. The ankle joint adopts a passive driving scheme, which is to fully exploit the passive dynamics of walking. This also contributes to the purpose of long endurance. Because if the LIPE's ankle joint is to achieve the power burst of normal walking, it will inevitably lead to an increase in the weight of the exoskeleton and large energy requirements, which may not be a desirable design idea.

The design of LIPE does not fully realize all 14 DOFs like human lower limbs because the more DOFs, the more complex the structure of the exoskeleton, which makes the control more difficult. To simplify the mechanical structure and the corresponding control strategy, we have abandoned several DOFs that has relatively little effect on the walking process, and finally determined that the LIPE has a total of 10 DOFs (5 per leg), which are the hip flexion/extension, ab/adduction and internal/external rotation, knee flexion/extension and ankle plantar/dorsal flexion.

Based on human anatomy and joint ROM, the joints of the lower limbs have certain limits of ROM due to the function of muscle ligaments. To fully ensure the safety of the wearer with the exoskeleton, the designed joints ROM are restricted to a range below the physiological movement of the human body. All joint angles are limited from the mechanical structure, sensor, and software level, respectively. The specific design values are shown in TABLE 3.

LIPE is supposed to accommodate the anatomical measures of 99% of the Chinese adult population, which dictates the wearer leg length and hip-width. These data come from the Human Dimensions of Chinese Adults, by taking the 1 and 99 percentile numbers [32]. With the same swing angle and time, the longer the leg length, the larger the actual step, and thus the faster the resulting walking speed. According to the available data, the maximal walking speed of similar products shown in TABLE 1 is around 0.5-0.8m/s except for Ekso (1.6m/s). Therefore, we used an average value of 0.6m/s as the target maximal walking speed of LIPE. To make users not to appear particularly strange during walking, we strive to improve the gait symmetry when wearing LIPE. The speed and other modes can be switched manually by pressing buttons on the forearm crutches.

C. Design and Implementation of LIPE's Torso Section and Hip Joint

The torso section of LIPE consists of a rigid backplate on which the control system and battery modules are integrated. LIPE attaches to the user at the torso and three places on each leg: the thigh, shank, and foot. At the torso, there are two shoulder straps and a pelvis strap that secure the user's torso to the rigid backplate.

From a kinematic point of view, the human hip joint can be regarded as a spherical pair. To achieve the same function on the exoskeleton, the hip flexion/extension and internal/external rotation are placed on the side, while the hip ab/adduction is moved to the back and connected to a rigid backplate. In addition, according to the size of the wearer's hips, the width and thickness of the LIPE can be adjusted (Fig. 1).

The actuators used in LIPE's hip joint applications should be compact, lightweight, and safe. Previous studies on the clinical gait analysis have recorded that the maximum power of

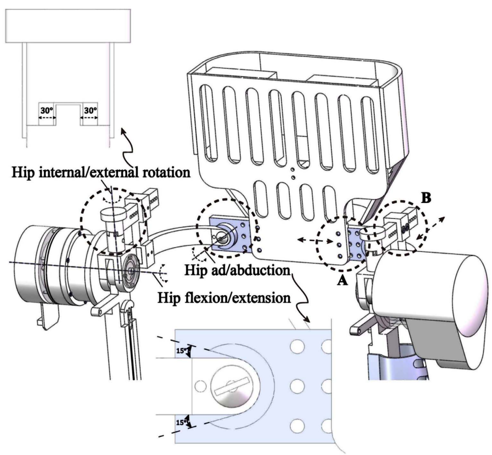

Fig. 1. The layout of 3 DOFs of LIPE's Hip joint. The hip flexion/extension is driven by the motor, while the other two DOFs are passive. A and B represent the width and thickness adjustment mechanism of LIPE's torso section, respectively.

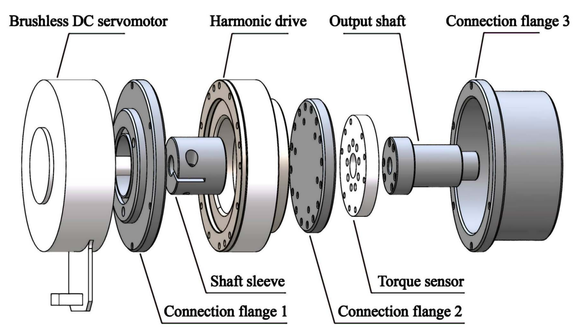

Fig. 2. The structure of the actuation system.

TABLE IV
THE PERFORMANCE OF THE ACTUATION PARADIGM OF THE HIP JOINT

Parameter	Unit	Actuation
Output nominal torque	Nm	73.12
Actuator mass	Kg	1.81
Actuator nominal torque density	Nm/kg	40.40
Control bandwidth (no load)	Hz	5.0
Backdrive torque	Nm	11.60

hip flexion/extension when a normal person walks at a speed of 1.0 m/s is about 80 W. The maximum torque is around 40 Nm [31]. We use this data to serve as a benchmark for the device. Therefore, two BLDC servomotors (Maxon EC90flat, Maxon motor AG, Switzerland) with a 160:1 reduction ratio harmonic drive (LHSG-20-160-C-I, Leaderdrive, Suzhou) are selected to be used in LIPE considering its compact design and safety against electrical hazards. At the same time, a small disc torque sensor (M2210E, Sunrise Instruments, Nanning) is integrated into the actuation system to detect the final output torque. The detailed specifications of the actuation system of the hip joint are shown in Fig. 2 and TABLE 4.

D. Design and Implementation of LIPE's Knee Joint

The human knee is a polycentric joint with a moving instantaneous center of rotation (ICR). The pathway of the successive ICR of the relative movement between the tibia and femur appears as a J-shaped curve on the sagittal plane [33]. The moving ICR contributes to the stability of the stance phase and the flexibility of the swing phase in a gait cycle. The knee joints of all exoskeletons mentioned in TABLE 1 above are uniaxial, namely that the knee ICR of these products is fixed. It is necessary to ensure that the exoskeleton and the human lower limbs do not move relatively during walking with the exoskeleton; this is likely to result in an unmatched knee ICR curve between the exoskeleton and the human in the sagittal plane, and further lead to unnatural gait. Therefore, a four-bar linkage mechanism, which widely used for prosthetic knee joints, is employed in the design of LIPE's knee joint. Since a number of similar works have been done in previous studies [34], [35], please refer to Appendix 1 for detailed parameter design of the four-bar linkage structure of LIPE's knee joint.

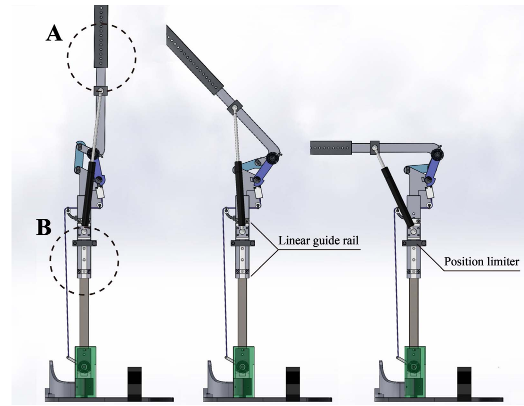

Fig. 3. The structure of LIPE's knee joint during the transfer between sitting and standing. A and B represent the adjustment mechanism of LIPE's thigh and shank segments, respectively.

The knee joint needs to bear a large torque during the transfer between sitting and standing. Therefore, a gas spring (310-100N, Shuangshan, Yangzhou) is integrated into the four-bar linkage knee joint to help the user complete such tasks. As shown in Fig. 3, to ensure that the gas spring can not only provide power assist in the posture transfer but also do not affect the gait, one end of the gas spring is hinged to the LIPE's thigh segment, and the other end is sliding connection with a fixed-length linear guide rail which attached to the shank segment. Therefore, the lower end of the gas spring can slide on the linear guide rail during level walking to not interfere with a normal gait. In addition, a position limiter can be manually opened to hold the gas spring on the fixed position of the guide rail and help users sit down and stand up.

Another issue to consider is the length of the linear guide rail. On the one hand, to prevent interference between the gas spring and the four-bar linkage during walking, it is necessary to ensure that the guide rail enables the knee joint to reach the limit angle of flexion/extension during normal walking. On the other hand, it should not be too long considering the weight and aesthetics. Clinical gait analysis data indicate that the maximum knee flexion angle is approximately 60 degrees for adults during level walking. According to this angle and the existing length parameters, the reasonable guide rail length is 105 mm.

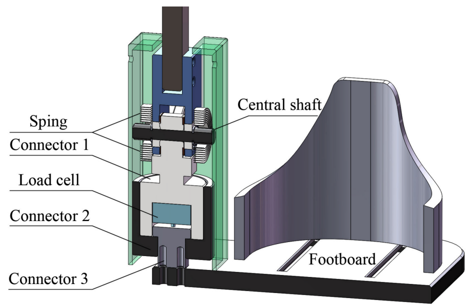

Fig. 4. Sectional structure of the LIPE's ankle joint.

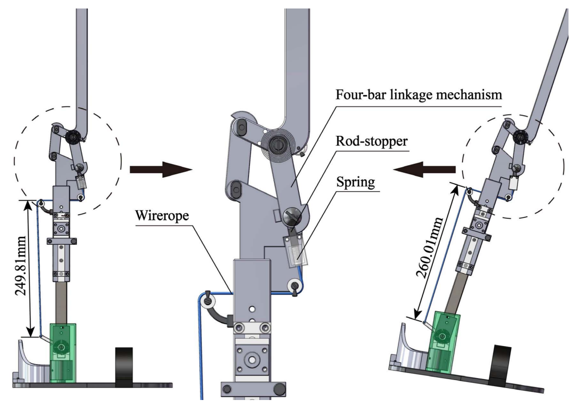

Fig. 5. LIPE's knee-ankle linkage mechanism.

E. Design and Implementation of LIPE's Ankle Joint

The LIPE's ankle joint is designed as a uniaxial rigid joint, namely the joint is coincident with the user's ankle joint and restricts rotation to dorsi/plantar flexion only. As shown in the sectional view of the ankle joint (Fig. 4), the plantar/dorsal flexion of the ankle joint rotates around a central shaft on which the spiral springs are attached at both ends. The neutral position of the spring is 0 degrees. A load cell (QLWH, QL Sensor, Bengbu) is integrated into the ankle joint to identify whether the exoskeleton is in a stance or swing phase.

In addition, the LIPE's knee joints should be locked for stability at the stance phase and unlocked for flexion like a normal human during the swing phase. Therefore, a knee-ankle linkage mechanism was proposed to realize such lock function, as shown in Fig. 5. The two sides of a soft wirerope were connected to the footboard and the rod-stopper, which attached to the rod of the knee joint, respectively. In the stance phase, the wirerope is slack, and the rod-stopper is supported up to lock the four-bar linkage mechanism of the knee joint by the spring. When ankle dorsal flexion is greater than 10 degrees in the swing phase, the wirerope will be tensioned to push the rod-stopper down for 10mm, which locked the four-bar linkage mechanism of the knee joint before. At the end of the swing phase, the plantar flexion releases the wirerope, and the spring pushes the rod-stopper to the groove of the four-bar linkage again, which locks the knee joint for stability in the next stance phase.

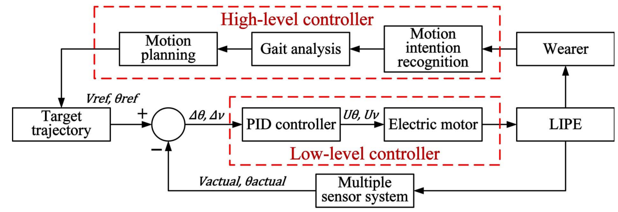

Fig. 6. Control architecture of LIPE. The function of the high-level controller is to generate reference trajectories for the exoskeleton according to the wearer's motion conditions, and that of the low-level controller is to regulate the actuators to output desired motions for the wearer.

F. Design and Implementation of Control System

In this study, the position control of predefined trajectory was adopted. The control structure shown in Fig. 6 incorporates a low-level controller and a high-level controller. The low-level controller is a PID control loop that uses joint angle and velocity feedback (in real time) to control the output of the joint motors to track the desired joint trajectories. The high-level controller is designed to recognize the wearer's motion intention based on the data collected by the multiple sensor system, analyze and evaluate the wearer's motion conditions, and finally generate reference trajectories for the exoskeleton.

During the level walking of the wearer with LIPE, as the input of motion intention recognition, the data of hip joint angle and ankle joint pressure are fused to analyze the gait phase of the exoskeleton. This result is further compared with the preset motion threshold to determine the wearer's motion intention and make the LIPE execute the target trajectories (take corresponding gait pattern).

The modularized control strategies are adopted by LIPE to reduce the complexity of the central controller and realizes the high-speed control. Therefore, five parts are integrated into the LIPE's control system, namely power module, main control panel, man-machine interface (MMI), sensor module, and motor drive module. The general control framework of LIPE is shown in Fig. 7.

The power module provides a power supply to the main control panel, the actuators, and all sensors. The 24V lithium-polymer battery is reduced to 12V and 5V through the DC-DC step-down circuit, and a fixed 3.3V output is further obtained through the low dropout (LDO) regulator, which can meet the voltage requirements of each module.

The main control panel, which adopts a 32-bit flash microcontroller (STM32F767IGT6, STMicroelectronics, Geneva), is the LIPE's brain to realize the walking function. It links each module, mainly responsible for data processing, intention identification, and motor control.

LIPE's human-machine interface includes the upper computer software and a manual control system embedded inside forearm crutches. The main controller receives the data of control information from the upper computer and executes it. The walking instructions are implemented by the manual control system. The control information is transmitted wirelessly to the power module and then to the main controller via controller area network (CAN) communication. Each crutch has two

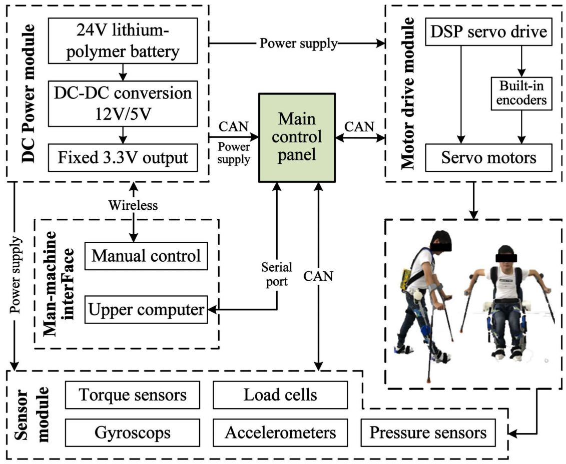

Fig. 7. Integrated control framework of LIPE.

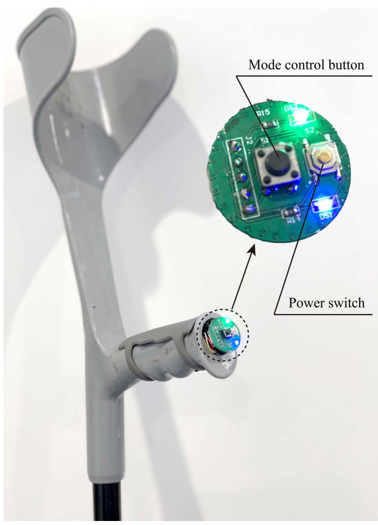

Fig. 8. The interface on the handle of the left crutch.

buttons on the handle (Fig. 8), one for the power switch and the other for the mode toggle. The wearer can manually control the trigger of each step by clicking the mode toggle button on the corresponding side or walk continuously by pressing the mode toggle button on both sides simultaneously according to their adaptability to LIPE. Similarly, the wearer can press the left mode toggle button for three seconds to sit down and the right to stand up.

Five types of sensors are used in LIPE to capture the wearer's walking characteristics. The inertial measurement units (IMUs) (JY901, Junyue, Shenzhen) are placed on the thighs, calves, and backplate, respectively. The sensor integrates accelerometers and gyroscopes, which can collect changes in attitude angle and the center of gravity during walking. The torque sensor in the actuation system (Fig. 2) is used to detect the moment change of the hip joint. The load cells at the ankle joint (Fig. 4) can determine the gait phase of the wearer when walking, that is, in the standing phase or the swing phase. Moreover, the pressure sensors are installed on the inner side of the crutch arm supports; they can identify

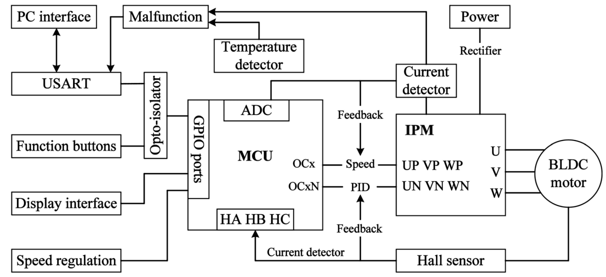

Fig. 9. The drive control schemes of LIPE.

the wearer's intention of walking by means of the difference between the left and the right pressure.

Before starting to walk, a quadruped stable state using the forearm crutches tilts the wearer's body forward so that the projection of the body's center of gravity on the horizontal plane is also tilted forward. When walking, the projection of the wearer's center of gravity alternates back and forth with the forearm crutches move forward and legs walk. These data will be collected by the above-mentioned IMUs.

LIPE adopts a strategy of personalized customization. The wearer must go through a training phase before using LIPE, in which a safe walking speed for the wearer will be initially determined. In continuous walking mode, the initial walking speed is based on the pre-selected safe walking speed. However, the strength of the upper limbs of different wearers is diverse; faster/slower moving forward of forearm crutches will lead to the projection of center of gravity of the wearer's body move faster/slower. This result is further compared with the preset motion threshold to determine the wearer's motion intention and make the LIPE execute the new target trajectories (take corresponding gait pattern).

The motor drive module is the power producer of the exoskeleton device, which includes the DC servo motor at the hip joint, the corresponding servo drive, and reducer. An encoder is integrated inside the servomotor to collect the position information of the motion and provides motion parameter feedback for the main control panel to realize closed-loop control. The servo drive control system adopted the intelligent power module (IPM) (PSS20S92F6, Mitsubishi, Japan), which integrated the drive and protection circuits. The microprogrammed control unit (MCU) used the 32-bit flash microcontroller (STM32F103RCT6, STMicroelectronics, Geneva) to achieve BLDC servomotor control. Fig. 9 illustrates the drive control schemes of LIPE.

The movement from sitting to standing with LIPE can be roughly regarded as a three-stage pattern: upper limbs support (mild hip extension), stand up (knee extension), and straighten up (hip extension). Similarly, from standing to sitting can also be divided into three phases: upper limb support (mild hip flexion), sit down (knee flexion), and straighten up (hip extension). Given there are large nonlinear changes in the beginning and end of the piston stroke [36], the gas spring in this study is only used to assist the wearer's posture transfer, which is independent of LIPE's control system. However, to make the entire process of posture transfer controllable, we adopted the strategy of early intervention and delayed exit

Fig. 10. A wearer with LIPE during walking and posture transfer.

TABLE V
BASIC DEMOGRAPHIC INFORMATION

Subject	Gender	Age(yrs)	Weight (kg)	Injury level	Post-injury time (yrs)
1	Male	30	72	T11	1.5
2	Male	45	67	L1	6

of the servomotor to ensure a smoother connection of the three stages.

Based on the above design requirements, the design plan was finalized after several discussions. Fig. 10 displays the prototype being worn at different postures. Two backpack braces and a pelvis brace are used to attach the LIPE to the upper body of the wearer. Two thigh braces are added to constrain the upper leg and support the user during standing up. Two shank braces are employed to support most of the weight of the wearer in standing and walking. Similarly, each footboard has two braces to attach the human foot. The prototype weighs around 13 kg and costs about eleven thousand dollars.

III. EXPERIMENTAL TASKS AND RESULTS

The proposed LIPE has been tested preliminary using several experiments, including level walking and posture transfer with two complete traumatic SCI patients. The Walking Index for SCI (WISCI II) of all subjects reached level 9 (Ambulates with walker, with braces and no physical assistance, 10 meters) or higher [37]. Before participating in this study, the two subjects used wheelchairs as assistive products for personal mobility. Two subjects volunteered and signed the written consent forms to participate in this study approved by the Institutional Review Committee of Shanghai University of Medicine & Health Sciences (2019-ZYXM1-04-420300197109053525, 10.07. 2019). The basic demographic information is shown in TABLE 5 below.

All experiments were performed in a laboratory environment, where a standard walkway was available. A safety harness worn by the wearer was attached to an overhead suspension system moving along with the wearer, which only came into action when the subject fell. Before the formal test, the subjects were required to attend two training sessions, including how to work with LIPE for level walking and posture transfer to fulfill the experimental task without difficulty. Each training session lasted around 1 hour. For each subject, the complete experimental session lasted 2 to 2.5 hours. In order to make the subjects safer and easier to control LIPE, all the following evaluations were conducted in the walking mode triggered by each step.

TABLE VI
THE WALKING PARAMETERS OF THE SUBJECTS

Subject	Leg length* (m)	Step length (m)	Step period (s)	Average walking speed (m/s)
1	0.82	0.40	2.35	0.17
2	0.77	0.36	2.57	0.14

* Distance from hip joint to ankle

A. Level Walking Evaluation

Level walking is one of the basic functions of LIPE. We used the 3D IMU-based motion capture and analysis system (MyoMotion, Noraxon, Arizona) to record the gait data of the subjects with LIPE at a frequency of 100 Hz (system default) and analyze their characteristics. For the data presented in the subsequent sections, the evaluation protocol was as follows.

The subjects were helped to put on the LIPE in a sitting position, and seven motion capture sensors were also attached to the pelvis, thighs, shanks, and feet of subjects, respectively. LIPE's torso, thigh, and shank segments were adjusted to appropriate lengths according to the subject's anthropometric data and then stood up by pressing the buttons on the crutches. The experiment could start after the sensors were calibrated. The joint angle can be displayed directly from the companion software MR3 (MyoMotion, Noraxon, Arizona). Each subject walked five gait cycles (about 8 meters) at the speed they felt most comfortable according to the training requirements in the trial. Considering the influence of the state change of the beginning and the end of the walk, we selected the data of the third gait cycle for analysis. Specific walking parameters of the subjects are shown in TABLE 6.

To make these data of different speeds comparable, Fig. 11 illustrates a comparison of the joint angles between the two subjects and an non-disabled person (70kg, walking speed 1m/s) in the Clinical Gait Analysis (CGA) normative gait database [38] while level walking over one gait cycle. The measured data of the two subjects were processed by a 5 Hz filter. The lack of data for the coronal and horizontal planes in the database allows only the angular variation of the hip, knee, and ankle in the sagittal plane to be shown in Fig. 11.

As shown in Fig. 11, the maximum hip flexion in the non-disabled person at the end of the swing phase was around 40 degrees, while the subjects 1 and 2 reached about 30 degrees and 21 degrees, respectively. In the non-disabled person, knee flexion was about 57 degrees in the middle of the swing phase, while in both subjects, knee flexions were about 40 degrees. The ankle dorsal flexions of the two subjects were similar to that of the non-disabled person. However, the subjects did not have obvious plantar flexion (the non-disabled person can reach approximately 15 degrees in the initial swing phase).

The similarity of such data to normal biomechanics (particularly considering the amplitude of hip flexion/

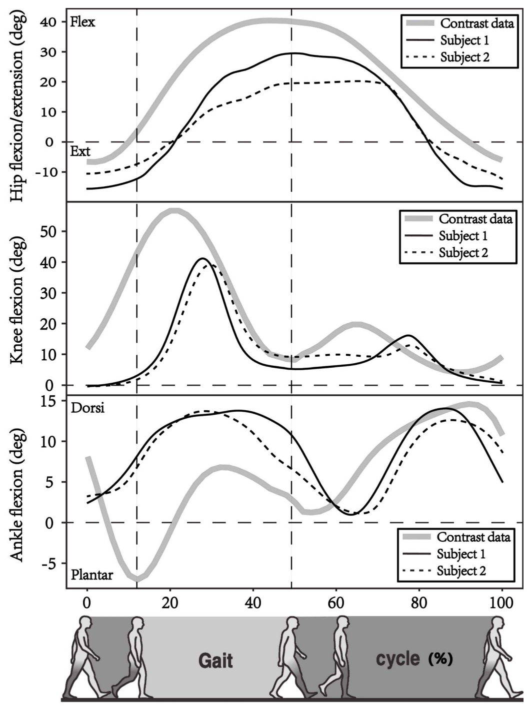

Fig. 11. Joint angles in the sagittal plane over one gait cycle. Light gray indicates the swing phase (around 40%) of a gait cycle, while dark gray indicates the stance phase (around 60%).

extension, knee flexion, and ankle plantar/dorsal flexion) indicates that the LIPE can provide appropriate gait assistance to the wearer during level walking. However, since the knee and ankle joints of LIPE are passive joints, the corresponding angles of the subjects are changed later than the contrast data. It also leads to the lack of obvious plantar flexion in the ankle joints of the subjects during walking.

Fig. 12 shows the measured angle data of the hip joint in the coronal and horizontal planes. According to the LIPE's technical requirements shown in TABLE 3, the amplitudes of the two angles are within the required range; this also implies that the function of level walking can achieve the design objective.

B. Posture Transfer Evaluation

Both putting on and taking off the LIPE require a sitting posture, so we further analyzed the torque provided by the actuator and gas spring as well as the angle change of the knee joint during posture transfer. The output torque at the hip joints and knee angle were read by means of the built-in sensors directly. Two IMUs (JY901, Junyue, Shenzhen) and a uniaxial force transducer (300kg, CGSENSOR, Henan) were employed to record the extension and force changes of the gas spring, respectively.

The posture transfer evaluation involved only the subject 1. He was asked to stand up independently from the chair and wait for his body to fully balance before sitting down. Repeat this for five cycles.

All data were recorded at a frequency of 20Hz and processed by a 5Hz filter. For comparison purposes, we present

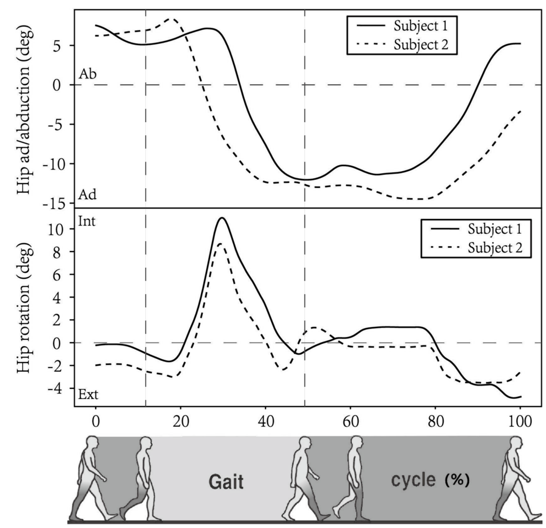

Fig. 12. Measured hip joint data of ad/abduction and external/internal rotation over one gait cycle. Light gray indicates the swing phase (around 40%) of a gait cycle, while dark gray indicates the stance phase (around 60%).

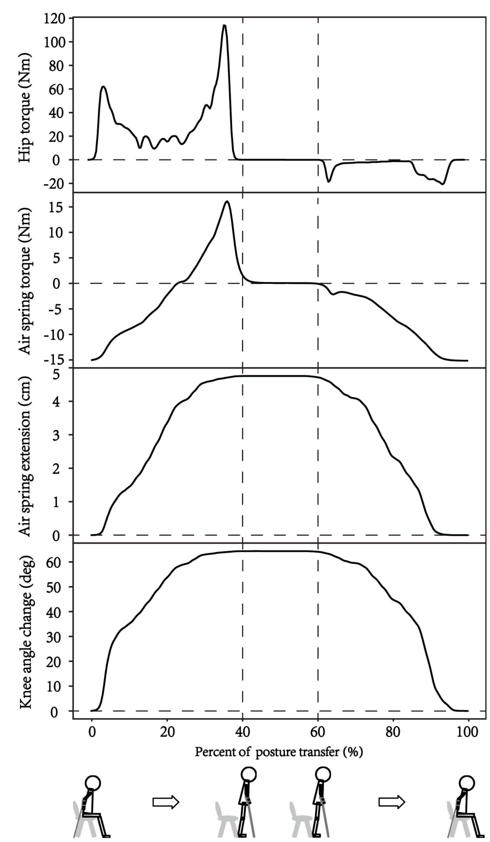

Fig. 13. Torque provided by actuator and gas spring as well as the angle change of the knee joint during posture transfer. The horizontal axis in the figure describes the percentage of posture transfer; 0 to 40% is from sitting down to standing up, 40% to 60% remains standing, and the rest represents standing to sitting down.

the data of sit-to-stand and stand-to-sit on one graph. Fig. 13 illustrates the data on one side of LIPE, 0 to 40% is from sitting down to standing up, 40% to 60% remains standing, and the rest represents standing to sitting down.

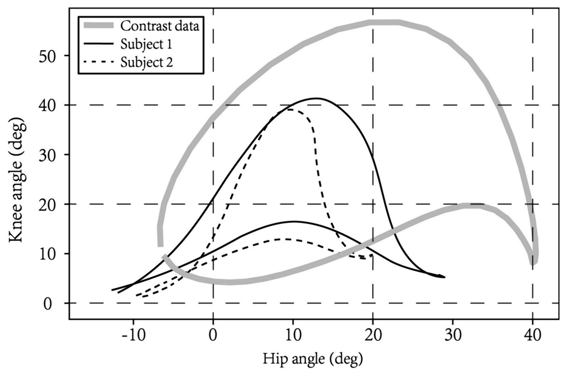

Fig. 14. Hip joint angle versus knee joint angle plot of the two subjects from walking tasks compared with the data in the CGA database. Data for one gait cycle is shown.

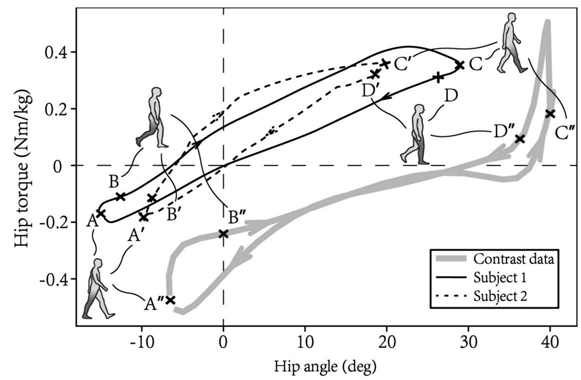

Fig. 15. The hip joint torque-angle data from the CGA database were compared with that of the two subjects who were wearing LIPE during level walking. X, X′, X″ (the letter “X” stands for A, B, C and D) represents the torque-angle data of subject 1, subject 2s and the CGA data at the same gait moment, respectively. A, B, C, and D corresponds to the beginning of the gait cycle, the beginning of the swing phase, the end of the swing phase, and the end of the gait cycle shown in Fig. 11, respectively.

It can be seen from Fig. 13 that the servomotor always intervenes earlier and exits later than the gas spring during the posture transfer, which can ensure the stability of the entire process. The torque of the actuator changes significantly as the hip angle changes. Moreover, as shown in Fig. 13, the hip output torque of the LIPE during the process from sitting to standing by the subject is greater than from standing to sitting because the former has to overcome the body gravity. The maximum compression of the gas spring is 48mm, and the peak torque was around 15Nm. In the late period from standing to sitting, since the moment applied to the gas spring reaches the maximum and the wearer’s upper limbs are no longer supported with crutches, the time from standing to sitting is shorter than from sitting to standing. In theory, the knee angle can be greater than 90 degrees when sitting down. However, the maximum angle change of the knee joint was 64 degrees during the test. This was probably due to the lack of strength in the lower limbs of the subject and the inability to resist the gas spring.

C. Kinematic Evaluation of the LIPE

Fig. 14 shows the plots of the hip joint angle versus the knee joint angle of the two subjects with LIPE performing the level walking task. This result was compared to the data above in the CGA normative gait database. It is clear from the plots that for the two subjects, the range of movement at both hip and knee is less than the contrast data. At the hip joint, the decrease in range is about 20%, and at the knee joint, the decrease in range is about 30%. For the individuals with the SCI, although the angle of the hip joint and the knee joint cannot reach the same level as that of an non-disabled person during the level walking, the experimental task can still be completed successfully. Moreover, the quadrupedal gait with forearm crutches causes the subject to lean forward when walking, so the hip and knee joint flexion angles of the subjects are smaller than normal.

The hip flexion/extension each leg of LIPE is powered, we further analyzed the relationship between torque and angle at the hip joints. The main gait cycle events can be identified on the basis of the contact between feet and ground; they are heel strike, contralateral toe off, contralateral heel strike, and toe off [39]. We plotted the hip joint torque versus joint angle and resulted in curves that were typical for each subject. Fig. 15 shows that the hip joint torque-angle data from the CGA database were compared with that of the two subjects who were wearing LIPE during level walking. As it appears, the hip joint torque-angle curve of an non-disabled person during level walking presents two loops: the first one (flexor moment) is counterclockwise, whereas the second (extensor moment) is clockwise [39]. However, the subjects involved have only a clockwise loop, namely the motors provide the extension moment. This is most likely related to the walking manners of the subjects while wearing LIPE. The quadrupedal gait with forearm crutches tilts their bodies forward so that the lower limbs are extended throughout the gait cycle, so the motor keeps providing flexor moment. In addition, we inferred from Fig. 15 that the upper limb participation of subject 1 was higher than that of subject 2. This is probably because he was younger, he had a shorter post-injury time and stronger upper limb strength, which allowed him to have more involvement of upper limb during the experiment.

In addition, we calculated the asymmetries of the hip and knee joints of the two subjects while wearing LIPE for level walking, which indirectly reflected the levels of gait symmetry of the subjects.

For each subject, asymmetries of the hip and knee joints were assessed using an improved symmetry index [40] defined as:

$$SI = \int_{t=t_1}^{t_2} \frac{2 \times |x_r(t) - x_l t|}{range\,[x_r(t)] + range\,[x_r(t)]} dt \tag{1}$$

where SI is the symmetry index, $x_r(t)$ is the value of a specific variable recorded for the right leg at the time t and $x_l(t)$ is the value recorded for the left leg at the time t. t_1 and t_2 represent the beginning and end of a complete gait cycle, respectively. The range $[x\,(\mathrm{t})]$ means the amplitude of $\mathrm{x}\,(t)$ at the time t. The integrand of Eq. (1) is referred to as the symmetry function and provides information on the time dependency of symmetry over the measured data during the

TABLE VII
THE SI VALUES OF HIP AND KNEE JOINTS FOR THE TWO SUBJECTS

Subject	SI_{hip}	SI_{knee}
1	0.77	0.68
2	0.85	0.88

experimental task. For any given variable, the closer the SI value approaches zero, the more symmetrical the gait.

Based on the obtained joint angle data and Eq (1), the SI values of hip and knee joints for the two subjects is shown in TABLE 7.

The results in TABLE 7 above illustrates that the gait of the subjects is somewhat asymmetrical when wearing LIPE, especially that of subject 2. This was most likely due to the control mode of each step and excessive use of their actual asymmetrical upper limbs' strength during the experiment. Nevertheless, as people with paraplegia, they completed all the experimental tasks, and the calculated SI values were below 1.0 (low asymmetry) [40] in the experimental protocol. Therefore, these results are acceptable.

D. Battery Life Evaluation of the LIPE

Long endurance is an important design requirement for LIPE. According to the battery parameters (24V, 10-15A, 10AH) we selected, the wearer of about 70kg should theoretically walk for around five hours at a uniform speed without interruption. We tested its actual performance specifically.

We built a test platform that can be adjusted between 50kg and 100kg. To simulate paraplegic subjects, the platform has the same DOFs as lower limbs, and all joints are non- powered. We set the platform weight to 70kg, fitted the LIPE and placed them together on the treadmill. They were then tilted forward about 12 degrees before being fixed on the shelf, in order to restore the state of the lower limbs in the quadrupedal gait, and to ensure that the footboards was always in contact with the treadmill. A battery capacity display was used to monitor the power in real-time.

The test uses continuous walking mode. After 4.5 hours of continuous walking at a speed of 0.6m/s, the display showed that 3% of the remaining battery was still available. This meets the needs of a light user to walk for one day.

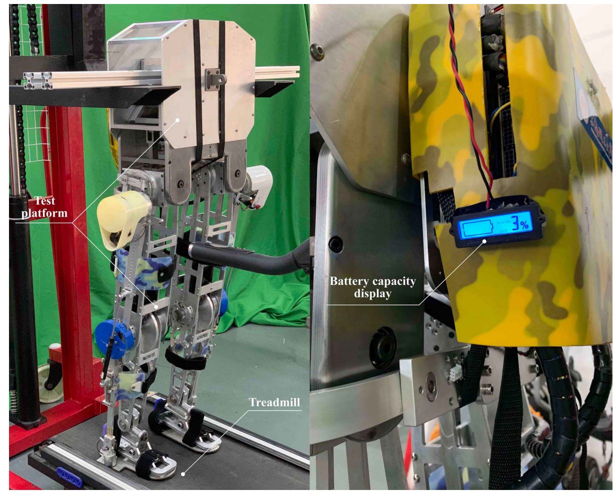

Fig. 16. After 4.5 hours of continuous walking, the display showed that 3% of the remaining battery was still available.

IV. DISCUSSION

This research proposed a lightweight powered exoskeleton during level walking for persons with paraplegia. We conducted a pilot study to examine our initial design goals as well as to evaluate LIPE's clinical function in practice. The LIPE consists of the torso section, hip joint, knee joint, ankle joint, thigh, and shank segments. This exoskeleton provides supportive and locomotive assistance for lower limbs. People with paraplegia can use it to walk and transfer sitting/standing posture independently.

The LIPE's development was a human-centered design process. A multidisciplinary design group including designers, users and physicians/occupational therapists, etc., participated in the entire design and experiment phases. The design of this exoskeleton stemmed from real user requirements; among them, many requirements such as lightweight, long endurance, and adjustability, etc., are related to the structure of the exoskeleton. The powered hip joint, four-bar linkage of the knee joint, and knee-ankle linkage mechanism not only realizes the purpose above but also make the functionality of LIPE was verified in experimental tasks. The structure is, therefore, more concise, compact, and lightweight than that in mentioned research [11], [14], [16], [23], [27]–[29]. The next generation of the exoskeleton is expected to be less than 10 kg by improving materials and processing technology.

Most of the lower limb exoskeletons in existing studies are used in conjunction with the forearm crutches. They are controlled by buttons on the crutches to achieve expected movements, such as continuously walking/stopping or standing/sitting [5], [11], [12], [14], [16], [17], [21], [22], [24]–[29]. For a user who has become accustomed to using the lower limb exoskeleton, the pattern of continuous walking may not be an obstacle. However, for people with paraplegia who are out of a wheelchair for a short time, individual control of each step is likely to be a better and safer option. All of LIPE's walking patterns can be achieved by using the two buttons on the forearm crutches, without the need for other supporting control terminals (such as wrist controllers or mobile phone APPs).

The combined results of our pilot study proved that the presented LIPE can provide a repeatable gait during level walking with knee and hip joint amplitudes that are similar to those data of the non-disabled person in the CGA normative gait database. This fully meets the requirements of a lightweight, powered, simple, and easy-to-use lower-limb exoskeleton for level walking and posture transfer. Meanwhile, it also has a long endurance of about 4.5 hours. It will be a promising way to help people with paraplegia gain some independence in daily life. And more importantly, its price is easily accepted by the users. The results encourage a further clinical functional evaluation of the users benefiting from the LIPE with more subjects in future research.

It is worth mentioning that we did not conduct experiments on LIPE's knee alone. Still, the research of four-link mechanism in the field of prosthesis has proved that it can make LIPE's knee joint movement closer to the real lower limb [41], so that the wearer can maintain better synchronization with the exoskeleton when level walking. In addition, the subjects' feedback on the operation of LIPE is relatively positive. Therefore, no experiments on energy consumption when walking with LIPE were conducted. We will focus on this aspect in the following research.

Some extensions and improvements, such as optimization of overall structure, could be considered in the next-generation LIPE. For instance, the torso section, thigh, and shank segments can be lighter and more fit to the human body under the premise of ensuring strength. The footboard should be shrunk and put into the shoes, which also narrows the difference from normal people, greatly reduces the weight and increases the endurance ability. In addition, we will try to make the LIPE's interaction more diversified and find a balance between functionality and cost. In future research, multi-channel feedback when wearing LIPE will also be considered.

V. Conclusion

Upright-legged locomotion is a desirable ability for all people with paraplegia. From the perspective of the user, a powered exoskeleton LIPE has been introduced that allows wearers to use it continuously for a long time. It is lightweight, cost-effective, easy to use, and especially practical for people with paraplegia in their daily lives. Moreover, the experimental results of the wearers shown that these subjects received the exoskeleton intervention well, and the LIPE could provide appropriate gait assistance to the wearer during level walking; it could also help the wearer achieve the posture transfer from sitting to standing or from standing to sitting independently.

Abbreviations

PD	Proportional-derivative.
PID	Proportional–integral–derivative.
IHMC	Institute for Human and Machine Cognition.
DOF	Degree of Freedom.
BLDC	Brushless Direct Current.
AIT	Asian Institute of Technology.
DC	Direct Current.
CSIC	Spanish National Research Council.
ZJU	Zhejiang University.
USWR	University of Social Welfare and Rehabilitation Science.
IRGO	Isocentric Reciprocating Gait Orthosis.
TU-Delft	Delft University of Technology.
MU	Mahidol University.
Fujita-HU	Fujita Health University.
NEU	Necmettin Erbakan University.
EPFL	Federal Institute of Technology Lausanne.
CUHK	Chinese University of Hong Kong.
THU	Tsinghua University.

Disclosure Statement

The authors report no conflicts of interest. The authors alone are responsible for the content and writing of this article.

References

[1] L. A. Harvey, R. Adams, J. Chu, J. Batty, and D. Barratt, "A comparison of patients' and physiotherapists' expectations about walking post spinal cord injury: A longitudinal cohort study," *Spinal Cord*, vol. 50, no. 7, pp. 548–552, Jul. 2012.

[2] C. F. Kunkel *et al.*, "Effect of 'standing' on spasticity, contracture, and osteoporosis in paralyzed males," *Arch. Phys. Med. Rehabil.*, vol. 74, pp. 73–78, Jan. 1993.

[3] M. O. L. Phillips, P. Axelson, J. Fonseca, *Spinal Cord Injury: A Guide for Patient and Family*. Skinidin, U.K.: Raven Press, 1987.

[4] R. A. Cooper, M. L. Boninger, R. Cooper, S. G. Fitzgerald, and A. Kellerher, "Preliminary assessment of a prototype advanced mobility device in the work environment of veterans with spinal cord injury," *NeuroRehabilitation*, vol. 19, no. 2, pp. 161–170, Jun. 2004.

[5] A. K. Raj, P. D. Neuhaus, A. M. Moucheboeuf, J. H. Noorden, and D. V. Lecoutre, "Mina: A sensorimotor robotic orthosis for mobility assistance," *J. Robot.*, vol. 2011, Oct. 2011, Art. no. 284352.

[6] N. Aphiratsakun and M. Parnichkun, "Balancing control of AIT leg exoskeleton using ZMP based FLC," *Int. J. Adv. Robotic Syst.*, vol. 6, no. 4, pp. 319–328, Dec. 2009.

[7] D. Sanz-Merodio, M. Cestari, J. C. Arevalo, X. A. Carrillo, and E. Garcia, "Generation and control of adaptive gaits in lower-limb exoskeletons for motion assistance," *Adv. Robot.*, vol. 28, no. 5, pp. 329–338, Mar. 2014.

[8] W. Yang, C.-J. Yang, and Q.-X. Wei, "Design of an anthropomorphic lower extremity exoskeleton with compatible joints," in *Proc. IEEE Int. Conf. Robot. Biomimetics (ROBIO)*, Dec. 2014, pp. 1374–1379.

[9] N. Costa and D. G. Caldwell, "Control of a biomimetic 'soft-actuated' 10DoF lower body exoskeleton," in *Proc. 1st IEEE/RAS-EMBS Int. Conf. Biomed. Robot. Biomechatronics*, Feb. 2006, pp. 495–501.

[10] M. Arazpour *et al.*, "Design and simulation of a new powered gait orthosis for paraplegic patients," *Prosthetics Orthotics Int.*, vol. 36, no. 1, pp. 125–130, 2012.

[11] S. Wang *et al.*, "Design and control of the MINDWALKER exoskeleton," *IEEE Trans. Neural Syst. Rehabil. Eng.*, vol. 23, no. 2, pp. 277–286, Mar. 2015.

[12] W. Banchadit, A. Temram, T. Sukwan, P. Owatchaiyapong, and J. Suthakorn, "Design and implementation of a new motorized-mechanical exoskeleton based on CGA patternized control," in *Proc. IEEE Int. Conf. Robot. Biomimetics (ROBIO)*, Dec. 2012, pp. 1668–1673.

[13] S. Tanabe, S. Hirano, and E. Saitoh, "Wearable power-assist locomotor (WPAL) for supporting upright walking in persons with paraplegia," *NeuroRehabilitation*, vol. 33, no. 1, pp. 99–106, Oct. 2013.

[14] U. Önen, F. M. Botsalı, M. Kalyoncu, M. Tınkır, N. Yılmaz, and Y. Şahin, "Design and actuator selection of a lower extremity exoskeleton," *IEEE/ASME Trans. Mechatronics*, vol. 19, no. 2, pp. 623–632, Apr. 2014.

[15] A. Tsukahara *et al.*, "Restoration of gait for spinal cord injury patients using HAL with intention estimator for preferable swing speed," *IEEE Trans. Neural Syst. Rehabil. Eng.*, vol. 23, no. 2, pp. 277–286, Oct. 2015.

[16] T. Vouga, R. Baud, J. Fasola, M. Bouri, and H. Bleuler, "TWIICE—A lightweight lower-limb exoskeleton for complete paraplegics," in *Proc. Int. Conf. Rehabil. Robot. (ICORR)*, Jul. 2017, pp. 1639–1645.

[17] B. Chen *et al.*, "A wearable exoskeleton suit for motion assistance to paralysed patients," *J. Orthopaedic Transl.*, vol. 11, pp. 7–18, Oct. 2017.

[18] Y. Li *et al.*, "Design and preliminary validation of a lower limb exoskeleton with compact and modular actuation," *IEEE Access*, vol. 8, pp. 66338–66352, 2020.

[19] Q. Ma, L. Ji, and R. Wang, "The development and preliminary test of a powered alternately walking exoskeleton with the wheeled foot for paraplegic patients," *EEE Trans. Neural Syst. Rehabil. Eng.*, vol. 26, no. 2, pp. 451–459, Feb. 2018.

[20] Cyberdyne. (2019). *HAL for Medical Use (Lower Limb Type)*. Assessed: Apr. 10, 2019. [Online]. Available: https://www.cyberdyne.jp/english/products/LowerLimb_medical.html

[21] ReWalk Bionics. (2019). *ReWalk: More Than Walking*. Assessed: Apr. 10, 2019. [Online]. Available: https://rewalk.com/rewalk-personal-3/

[22] Ekso Bionics. (2019). *Gait Train With EksoGT*. Assessed: Apr. 10, 2019. [Online]. Available: https://eksobionics.com/eksohealth/ eksogt/ patients/

[23] REX Bionics. (2019). *REX is a Hands-Free Robotic Device for Rehabilitation*. Assessed: Apr. 10, 2019. [Online]. Available: https://www.rexbionics.com/product-information/

[24] SuitX. (2019). *PHOENIX Medical Exoskeleton*. Assessed: Apr. 10, 2019. [Online]. Available: https://www.suitx.com/phoenix-medical-exoskeleton

[25] Indego. (2019). *Indego Personal Features*. Assessed: Apr. 10, 2019. [Online]. Available: http://www.indego.com/indego/en/Indego-Personal

[26] T. Gurriet *et al.*, "Towards restoring locomotion for paraplegics: Realizing dynamically stable walking on exoskeletons," in *Proc. IEEE Int. Conf. Robot. Autom. (ICRA)*, May 2018, pp. 2804–2811.

[27] Fourier Intelligence. (2019). *Fourier X2 Lower-Limb Exoskeleton Robot*. Assessed: Apr. 10, 2019. [Online]. Available: http://www.fftai.com/product_en/X2.php

[28] Ai-Robotics. (2019). *AiLegs*. Assessed: Apr. 10, 2019. [Online]. Available: https://www.ai-robotics.cn/products/ailegs

[29] RoboCT. (2020). *UGO*. Assessed: Oct. 22, 2020. [Online]. Available: http://www.roboct.com/products

[30] D. P. Losey, C. G. McDonald, E. Battaglia, and M. K. O'Malley, "A review of intent detection, arbitration, and communication aspects of shared control for physical human–robot interaction," *Appl. Mech. Rev.*, vol. 70, no. 1, pp. 1–11, Jan. 2018.

[31] C. Kirtley, *Clinical Gait Analysis-Theory and Practice*, R. Edwards, Ed. New York, NY, USA: Elsevier, 2006.

[32] *State Bureau of Technical Supervision. Human Dimensions of Chinese Adults*, Chinese Specification Press, Beijing, China, 1989.

[33] P. G. J. Maquet, *Biomechanics of the Knee: With Application to the Pathogenesis and the Surgical Treatment of Osteoarthritis*, 2nd ed. Berlin, Germany: Springer-Verlag, 1984.

[34] C. W. Radcliffe, "Four-bar linkage prosthetic knee mechanisms: Kinematics, alignment and prescription criteria," *Prosthetics Orthotics Int.*, vol. 18, no. 3, pp. 159–173, Dec. 1994.

[35] J. W. Michael, "Modern prosthetic knee mechanisms," *Clin. Orthopaedics Rel. Res.*, vol. 361, pp. 39–47, Apr. 1999.

[36] S. Zhang, L. Norum, and R. Nilssen, "Oscillatory motion application of tubular linear permanent magnet machine," in *Proc. 35th Annu. Conf. IEEE Ind. Electron.*, Nov. 2009, pp. 1223–1227.

[37] P. Dittuno and J. Dittuno, Jr., "Walking index for spinal cord injury (WISCI II): Scale revision," *Spinal Cord*, vol. 39, no. 12, pp. 654–656, Dec. 2001.

[38] C. Kirtley. CGA Normative Gait Database. Hong Kong Polytechnic Univ. Assessed: Aug. 3, 2014. [Online]. Available: http://www.clinicalgaitanalysis.com/

[39] C. Frigo, P. Crenna, and L. M. Jensen, "Moment-angle relationship at lower limb joints during human walking at different velocities," *J. Electromyogr. Kinesiol.*, vol. 6, no. 3, pp. 177–190, 1996.

[40] S. Nigg, J. Vienneau, C. Maurer, and B. M. Nigg, "Development of a symmetry index using discrete variables," *Gait Posture*, vol. 38, no. 1, pp. 115–119, May 2013.

[41] S. A. Gard, D. S. Childress, and J. E. Uellendahl, "The influence of four-bar linkage knees on prosthetic swing-phase floor clearance," *J. Prosthetics Orthotics*, vol. 8, no. 2, pp. 35–40, 1996.